(Received 2 February 2024, Accepted 9 March 2024, Scheduled 21 March 2024)

A Miniaturized and High-Gain Antipodal Vivaldi Antennas Using Directors

Islam M. Ibrahim[1,2], Mohamed I. Ahmed[3], Hala M. Abdelkader[1], Ahmed Jamal Abdullah Al-Gburi[4,*], and Moataz M. Elsherbini[1,2]

[1]*Department of Electrical Engineering, Shoubra Faculty of Engineering, Benha University, Cairo 11629, Egypt*
[2]*Department of Electrical Engineering, The Egyptian Academy for Engineering and Advanced Technology (EAEAT), Egypt*
[3]*Microstrip Department, Electronic Research Institute, El-Nuzha, Cairo 11843, Egypt*
[4]*Center for Telecommunication Research & Innovation (CeTRI), Faculty of Electronics and Computer Technology and Engineering Universiti Teknikal Malaysia Melaka (UTeM), Jalan Hang Tuah Jaya, Durian Tunggal, Melaka 76100, Malaysia*

ABSTRACT: In this paper, a miniaturized millimeter-wave (mm-wave) antipodal Vivaldi antenna (AVA) is proposed. The AVA antenna structure is modeled using MWSCST2022 optimization tools. The AVA exhibits good impedance matching, high gain, and a small optimum size of $5 \times 2.5 \times 1.5\,\text{mm}^3$, fabricated on an FR-4 substrate. An array of square and circular director units is modeled and loaded at the front and back of the AVA antenna. The spacing between directors is studied and positioned at a tuned distance from the antenna for gain improvements and optimum radiation parameters. The AVA has an operating spectrum from 58 GHz up to 62 GHz. The finalized AVA, along with directors, obtained a high gain of 12.9 dBi with directors, while the AVA achieved 9.22 dBi without directors. The proposed antenna model is simulated and measured for short-range communications and imaging. The results of the modeling techniques and measurements agree well with each other.

1. INTRODUCTION

Millimeter-wave (mm-wave) innovations have gained significant interest due to the steadily growing need for various applications in high-speed wireless networks, high-resolution imaging, automobile radars, and more. A broad spectrum offers advantages for the outstanding functionality, small size, and high interconnectedness required by these systems [1]. According to the literature study, many researchers investigated Vivaldi antennas with multiple bands: In [2], a metamaterial-based Vivaldi antenna with ultra-wideband and high gain can be used in ground-penetrating radar devices. The metamaterial comprises various "H"-shaped sections inserted at the top of the antenna aperture and directors packed within the antenna to enhance the gain. Edge grooving is combined with the practical approach of mounting a dielectric lens. Evaluation of the results reveals that the antenna performs well at 4 and 16 GHz [3]. Metasurface-coated Leaky-Vivaldi antenna (LVAM) operates in the 5G sub-6 GHz spectrum (3.3–5.3 GHz) and X band (8.0–12.0 GHz) with realized gains of 8.8–9.6 dBi and 11.8–15.2 dBi, respectively [4]. The antenna maintains effectiveness from 55 to 84 GHz, with a radiation efficiency exceeding 80% and a gain of 7 dBi [5]. For wireless communication devices, a coplanar waveguide (CPW) and photovoltaic cells were integrated, boasting a transparency rating of 63.3%. Crafted from Plexiglas with a dielectric value of 4.4, the antenna operates from 2 to 32 GHz [6]. Another 1×4 Vivaldi antenna array spans a broad frequency range of 6.3 GHz (10.78–17.07 GHz) with an optimal gain of 13 dBi at 15 GHz [7]. A compact, gain-enhanced Vivaldi antenna for 5G millimeter-wave applications with dimensions of $5.5 \times 12\,\text{mm}^2$ demonstrates an effective bandwidth of 22.5–45 GHz, covering 5G's spectrum up to 70 GHz [8]. A two-port AVA with graphene construction offers higher gain for THz purposes than traditional conductive copper, providing fully reconfigurable functionality from 3 to 4.5 THz [9]. A portable Vivaldi antenna, measuring $36 \times 36\,\text{mm}^2$ and utilizing FR-4 as the dielectric material, provides a gain of 8.5 dB across a frequency range of 3 to 10.6 GHz [10]. Results indicate an extended dual-polarized impedance spectrum of 20.04–25.5 GHz (23.97%) with gains of 5.2 and 8.2 dBi, highlighting effective utilization in wireless transmission [11]. A Vivaldi antenna, known for its distinctive large bandwidth and high gain, is suitable for various applications, such as microwave imaging, with a spectrum ranging from 1.5 to 55 GHz [12]. An AVA with parasitic patches and homogeneous corrugation has a size of $50 \times 86\,\text{mm}^2$ and a gain of 11.31 dBi. This antenna is utilized for breast cancer identification [13]. A broad-band log periodic dipole antenna (LPDA) with dimensions of $20 \times 40 \times 0.508\,\text{mm}^3$ and directors on a Roger's RT5880 substrate ($\varepsilon_r = 2.2$) achieves a frequency range from 26 to 44 GHz and a maximum gain of 14.29 dBi [14]. The Vivaldi antenna maintains a broad impedance range of $25:1$ between 2 GHz and 50 GHz, with a return loss less than -10 dB and a gain of 4–12 dBi [15]. Vivaldi antennas designed on an FR-4 dielectric surface, introducing a gain of about 9 dBi at 4 GHz within a range of 3 to 8 GHz, are used for ultra-wideband identification instruments [16]. Vivaldi antennas with dimensions of $45 \times 35 \times 0.79\,\text{mm}^3$ exhibit a gain of 10.2 dBi and a decent reflection coefficient over a

* Corresponding author: Ahmed Jamal Abdullah Al-Gburi (ahmedjamal@utem.edu.my), (ahmedjamal@ieee.org).

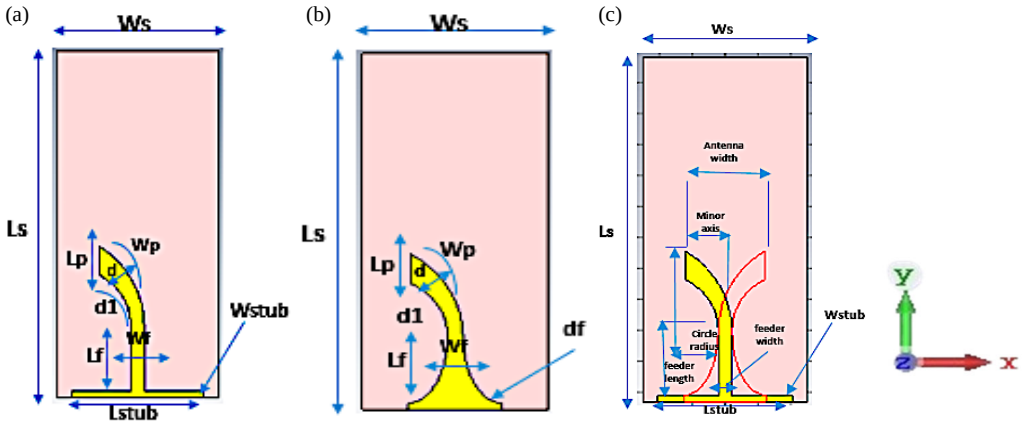

FIGURE 1. The proposed AVA Antenna model without directors, (a) front view, (b) back view, and (c) complete AVA model.

wide operational spectrum of 23.19 GHz, applicable to satellite applications [17]. A compact AVA radiating flare with rectangular slots enhances gain and reduces side lobe levels, achieving an enhanced gain of 3.8 dB and a front-to-back ratio exceeding forty dB at 20 GHz [18]. An ultra-wideband Vivaldi antenna suitable for drones operates from 3.1 to 10.6 GHz, reaching a maximum gain of 6.6 dBi at 9 GHz with a boosted bandwidth of 10.57 GHz (2.87–14.54 GHz) [19]. A small AVA and a dielectric lens achieve efficiency between 95.93% and 97.52%, operating among 24.17 GHz, 29.37 GHz, 30.76 GHz, and 40.58 GHz, used for 5G applications [20]. The performance of the Vivaldi antennas is enhanced by some approaches, like feeding mechanisms, integration of slots, dielectric material choice, and radiator shape. The performance of a Vivaldi antenna can be increased by including a dielectric lens, a parasitic patch in between two radiators, corrugations, and metamaterials [21]. In this sense, the contributions of this paper can be summarized as follows:

1. The paper introduces a miniaturized millimeter-wave AVA, addressing the challenge of size reduction in mm-wave applications, crucial for practical implementation in compact devices.

2. The AVA demonstrates desirable characteristics such as good impedance matching, high gain, and a small optimum size ($5 \times 2.5 \times 1.5\,\text{mm}^3$). Achieving these simultaneously is noteworthy, as it often involves trade-offs in antenna design.

3. The AVA operates in the frequency range of 58 GHz to 62 GHz. The article highlights significant gain variation with and without directors, showcasing the impact of the director units on the antenna's overall performance in the mm-wave spectrum.

In this paper, a miniaturized and high-gain AVA is proposed for mm-wave applications. The dimensions of the proposed AVA are $5 \times 2.5 \times 1.5\,\text{mm}^3$ and fabricated on a low-cost FR-4 substrate, while the electrical dimensions are $0.009\lambda_0 \times 0.004\lambda_0 \times 0.002\lambda_0$. The proposed AVA operated at frequencies from 58 up to 62 GHz, measuring a bandwidth of 4 GHz. It achieved a high gain of 12.9 dBi at the resonant frequency of 60 GHz. A small stub is modeled with the feeding line mechanism of the AVA for impedance matching.

2. PROPOSED ANTIPODAL VIVALDI DESIGN WITHOUT DIRECTORS

The presented engineered antipodal Vivaldi antenna layout is incorporated, simulated, and fabricated on the FR-4 material layer, as illustrated in Fig. 1. It has a relative permittivity around 4.4, $t = 0.035\,\text{mm}$. The electric conductivity of copper, which is a lossy metal, is $5.8 + \text{e}07$ s/m, and the dielectric substrate thickness is 1.5 mm. The antenna's dimensions of $5 \times 2.5\,\text{mm}^2$ make it appropriate for millimeter-wave applications shown in Table 1. At a resonance frequency of 60 GHz, the spectrum that can be generated by this antenna extends from 58 GHz through 62 GHz to fulfill the requirements for communication technologies. The feeder width for the antenna was adjusted to achieve the best matching at 50 ohm line impedance. The following equation defines the curves, repre-

TABLE 1. Optimized dimensions for antipodal Vivaldi antenna.

Symbol	Value (mm)
W_s	2.5
L_s	5
H	1.5
W_f	0.41
L_f	2.1
W_p	2.4
L_p	10
d_1	0.1
D	1.3760
D_f	0.9990
ε_r	4.4
L_{stub}	4.1
W_{stub}	0.2

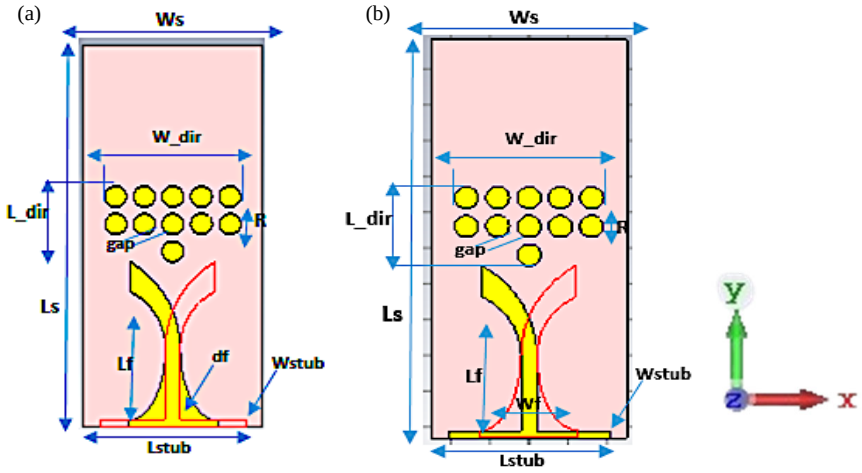

FIGURE 2. The proposed AVA model with circular directors, (a) front view, and (b) back view.

sented by R above, for two points along the curve, $A1(x1, y1)$ and $A2(x2, y2)$ [2]:

$$y = C1e^{RX} + C2 \quad (1)$$

$$C1 = \frac{y1 - y2}{e^{RX2} - e^{RX1}} \quad (2)$$

$$C2 = \frac{y2e^{RX2} - y1e^{RX1}}{e^{RX2} - e^{RX1}} \quad (3)$$

The high frequency F_H is set using the values $C1, C2$, and the opening rate R, which are ascertained by Equations (1) and (2) and Equation (3). Following the creation of each of these forms, the flare is obtained by connecting the feed rectangle and deducting the circle from the ellipse [22]. There will also be some leftover, unwanted forms that should be discarded to the left of the feed line and beyond the bounds of the substrate. The final step involves placing the ground flares at the top and bottom of the substrate. Vivaldi antennas offer a number of advantages over other topologies. The antenna's gain can be easily increased by expanding the substance across the radiating aperture in the role of a dielectric director.

3. PROPOSED LOADED ANTIPODAL VIVALDI DESIGN WITH CIRCULAR DIRECTORS

The foremost objective of our present work is to maximize the antenna functionality. The prototype in Fig. 1 is equipped with a small director unit with optimized dimensions above the antenna to maximize the gain, as in Fig. 2. The directors are designed as a circular patch with optimized and small dimensions, as shown in Table 2, to replace dielectric lenses and metamaterials in order to maximize gain. The directors were a little shorter and added at the front of the antenna with tuned spacing. The directors have a progressive lagging current phase that will increase the gain of the antenna by reradiating the electromagnetic waves with a new phase; they change the radiation patterns of the waves. Because of this constructive interference, this strengthens the overall signal and, consequently, lowers side lobes and raises gain. On the other hand, metamaterials stimulate new perspectives on traditional electromagnetic concepts. The metamaterial structure's resonant characteristics and some of the resulting bandwidth limitations are the main drawbacks. Metamaterial-inspired antennas frequently have low gain. The challenges stem from the resonant characteristics of the metamaterial structures and the consequent limitations in bandwidth. Metamaterials are lossy, have a limited wavelength range of operation, are difficult to produce in large quantities, and are unable to change shape while in use. In order to achieve high gain and a broad spectrum in smaller dimensions for use in portable and modern communications systems, the antenna was developed in the shape of an antipodal Vivaldi antenna. An end-fire antenna is used in this situation, and it is anticipated that it will offer high gain, few side lobes, and a broad bandwidth. These antennas are excellent for applications involving short-range wireless communications and imaging. It is inexpensive, has a consistent radiation pattern, is physically simple, and loses less energy. The antipodal feed approach, which maintains the antenna spectrum wide and its input impedance low, is one quick and efficient approach to feeding Vivaldi antennas. The antenna operates when the feeding line W_f, which might be concluded with a sector-shaped region or a direct coaxial connection, activates an open space through a microstrip line.

3.1. Parametric Study for AVA with Circular Directors

Due to the perceptive influence of director units after great parametric studies, circular directors receive backing for the AVA, as revealed. Since the current created on the arms is better suited for wave propagation than radiation, it is possible to attain the same radiation performance. Fig. 2 shows the compact AVA design with director units. Plain directors are included as a grid with dimensions in Table 2 in front of the antenna to boost gain while simultaneously enhancing efficiency. The separation between the director elements and the overall diameter of the director are both regulated for better radiation and gain amplification. Directors are made to take the place of metamaterials and dielectric lenses in order to obtain more benefit by improving a director's impact. Antennas based on metamaterials usually have improved gain. The circular sym-

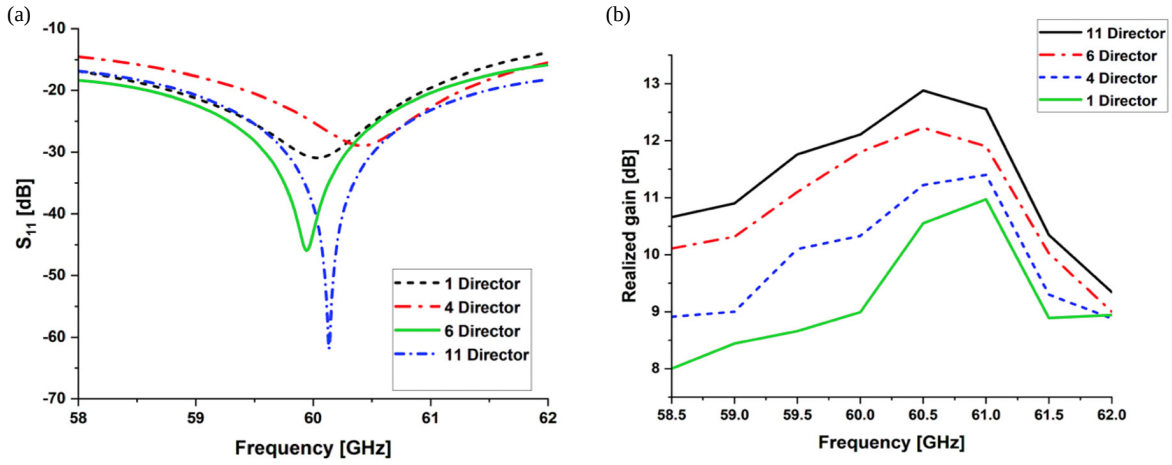

FIGURE 3. Parametric study results for AVA antenna with circular directors, (a) S_{11}, and (b) realized gain (dBi).

Table 2. Optimized dimensions for circular directors.

Parameter	Value (mm)
R	0.6
$W_$dir	3.8
$L_$dir	2.2
Gap	0.2
r	0.3

Table 3. Optimized dimensions for square directors.

Parameter	Value (mm)
L	0.4
$W_$dir	4
$L_$dir	2.2
Gap	0.2
r	0.3

metrical director elements are designed as a circle patch with a radius of 0.3 mm and placed along the antenna Y-axis at a determined distance with extensive parametric study to have an optimized displacement tuned with the antenna. The gaps among the director components are symmetrical and studied to be 0.2 mm. The director's width above the antenna is 3.8 mm, and its length is 2.2 mm. Also, S_{11} is improved, and the matching is enhanced with the increase in the number of directors. The parametric study of S_{11} also affects the number of directors, as shown in Fig. 3(a). For six and twenty directors, the antenna has the best optimized S_{11} at -46.5 dB and -65.2 dB. Parameter sweep starts at first with one director above the antenna on the front and back sides. The gain increased from 9.22 dBi of simulation to 8.77 dBi for the measured value without loaded directors, as shown in Fig. 1. The directors increased to form four directors, and there is another change and an increase in the realized gain to be 11.22 dBi. Repeatedly, the director increased to six, and the gain reached 11.55 dBi. Then, we duplicated the director numbers, which reached 13 directors, so the gain improved to 11.96 dBi. Finally, when the number of directors is duplicated to 20, the enhanced realized gain becomes 12.44 dBi, as illustrated in Fig. 3(b). As a result, it is concluded that the numerous director elements make the antenna's radiation characteristics better than those of an unloaded one.

4. PROPOSED LOADED ANTIPODAL VIVALDI DESIGN WITH SQUARE DIRECTORS

With the same AVA as shown in Fig. 1, a square-shaped director is utilized on the Y-axis of the design at a tuned distance determined by numerous parametric studies to find the optimum spacing between the antenna and the director units. The director is a square patch with a size of $0.2\,\text{mm} \times 0.2\,\text{mm}$, as illustrated in Fig. 4. The director dimensions are listed in Table 3. The gain is enhanced by increasing the number of directors. The first row includes 1 director at the front and back views of the antenna, and we noticed that the realized gain improved. The number of directors is doubled to form the second row, which includes five directors, but the gain is still increased. The finalized value for the gain reached 12.9 dBi significantly with adding the directors to 20 units.

4.1. Parametric Studies for AVA with Square Directors

The directors are discretely positioned on both sides of the antenna and separated symmetrically. The gain in the antenna bandwidth only marginally increases when this configuration is modeled with just one pair of directors placed far from the antenna at an optimal dispersion among directors. It has been shown that at the highest frequency, the gain grows properly. To improve the gain and matching of the antenna, the directors were made in the shape of a square $0.2\,\text{mm} \times 0.2\,\text{mm}$, as shown in Fig. 4. To figure out how to get the greatest gain and matching through a combination of trial and error techniques until we reached the most optimal positioning, a thorough investigation of this separation between the antenna and directors was conducted. We were capable of going a distance shorter than that because of fabrication restrictions, despite the fact that the lowest size that can be built when the masks are created is 0.2 mm. Directors were added to the antenna's back layer since it was obvious that their presence increased gain. This led to the inclusion of more directors, which also increased the gain. The film makers alter the metamaterial and lens. The effects of a

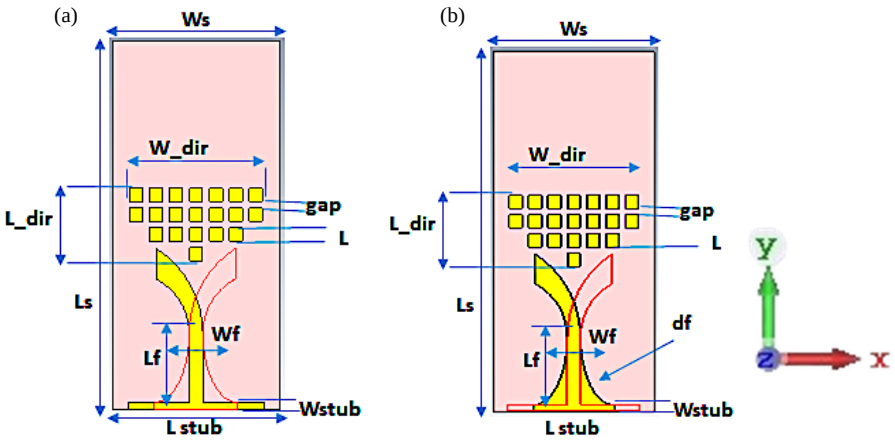

FIGURE 4. The proposed AVA antenna model with square directors, (a) front view, (b) back view.

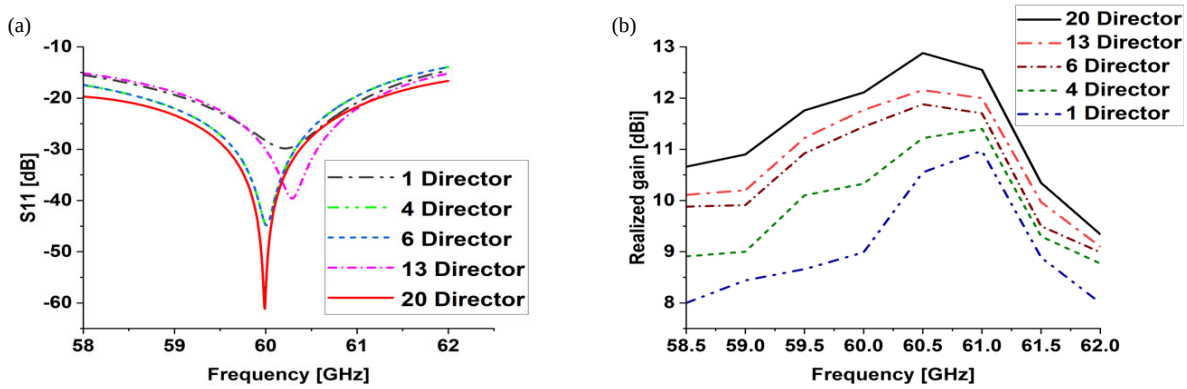

FIGURE 5. Parametric study results for AVA with directors, (a) S_{11}, and (b) realized gain (dBi).

key parameter on the gain, bandwidth, and SLL were investigated using a variety of parametric tests on the MWSCST 2020. The directors also affect the S_{11}; while one director is used, the return loss reaches -29.818 dB. The director was duplicated to four and six director units, and the S_{11} changed greatly to -44.82 dB. However with thirteen directors, the S_{11} becomes -39.89 dB, and there is a slight shifting in the S_{11}, but still a good matching. Finally, with 20 directors, S_{11} improved until it reached 64.73 dB, as shown in Fig. 5(a). The sequence of directors in both the front and back was built after the overall number of directors climbed from one, and the gain reached 8.77 dBi, then four, so the gain was enhanced to 10.12 dBi. The gain is still increasing toward the director number, and the gain reaches 12.9 dBi with the effect of 20 directors in Fig. 5(b).

5. RESULTS AND DISCUSSIONS

According to the attractive analysis for the implemented AVA, an accurate representation of the planned performance of the AVA is attained. The purpose of the antenna fabrication procedure was to verify the actual functioning and corroborate the previously demonstrated outcomes of the simulation. The reflection coefficient reached -46.5 dB for simulation and was measured at -36.33 dB without director units. Furthermore, the S_{11} values are -62.8 dB for simulation and -34.701 dB for measurements with circular-shaped directors. Last but not least, the S_{11} was enhanced greatly by using a square director of -64.73 dB for modeling and an approximate of -54.569 dB for measurements, which is obvious in Fig. 6(a). This shows the modest variations in the measured value due to the fabrication environment and material parameters. While return loss is maintained since the directors are added to enhance gain and radiation pattern enhancement at the operating frequency bandwidth, the size of parasitic elements must be improved. The loaded AVA with directors achieved an enhancement in the gain about 3.68 dBi. It is noticed that the realized gain for AVA without directors reached 9.22 dBi and 8.77 dBi for modeling and measurements, respectively. The antenna is promoted by adding 11 circular director units, so the gain is raised to 12.33 dBi for simulation, compared to the measured value of 11.96 dBi with a circular director. The peak gain improved to 12.9 dBi using square director elements, as shown in Fig. 6(b). The implemented antennas are shown in Fig. 7. The S_{11} of the built-in AVA was measured using a Vector Network Analyzer VNAZ67 with a port impedance of 50 ohm, as obvious in Fig. 8. The antenna has the best characteristics between the proposed work and the previous designs listed in Table 4. The loaded antennas with directors have a better reflection coefficient, greater gain, better and more stable radiation pattern, and lower side lobes than the unloaded ones, improving the performance and antenna efficiency.

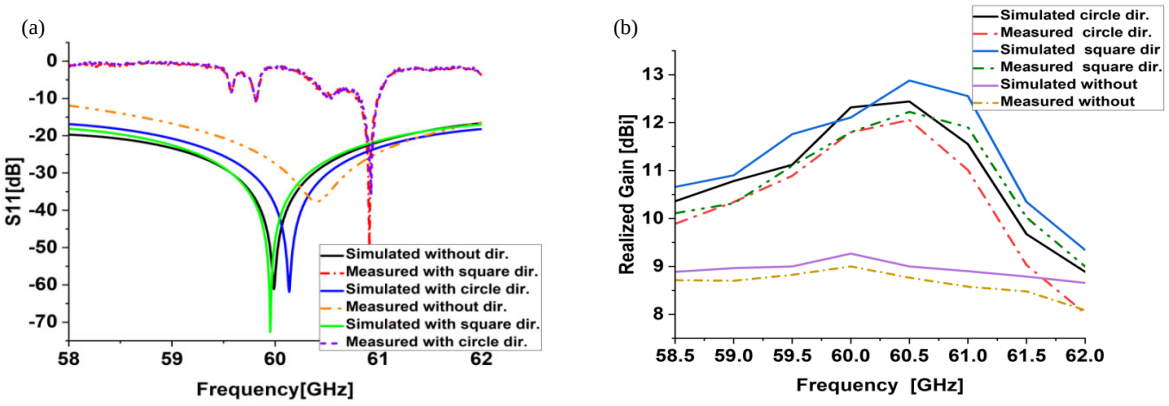

FIGURE 6. Simulated and measured results of the finalized AVA antenna with and without directors, (a) S_{11} and (b) realized gain.

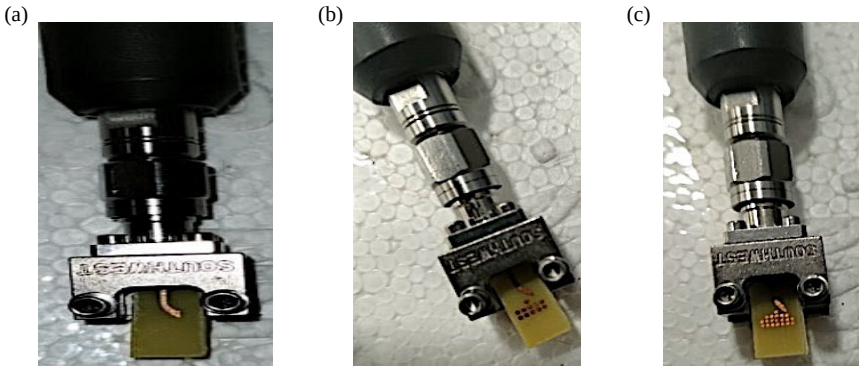

FIGURE 7. Fabricated prototypes, (a) AVA antenna without, (b) AVA antenna with circular director, (c) AVA antenna with square director.

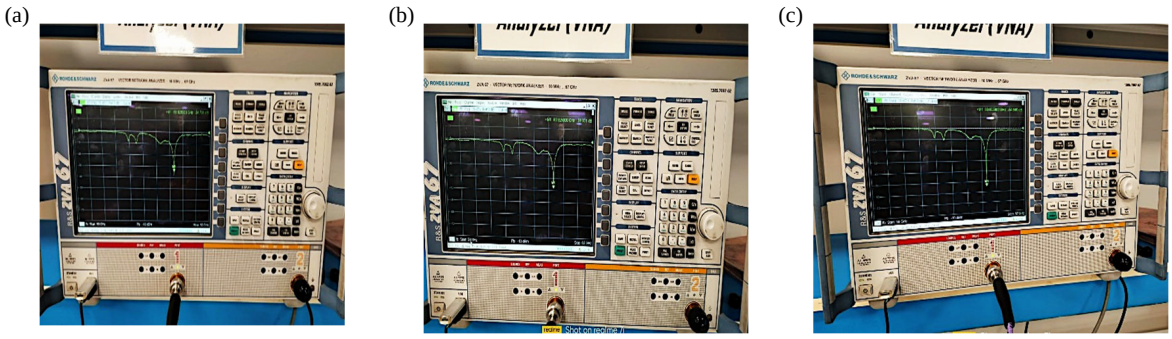

FIGURE 8. Measured S_{11} using VNA, (a) without director, (b) with circular director, (c) with square director.

The gain of the AVA was calculated using the radiation pattern measurements. Two equivalent horn antennas put up in an aligning configuration that was line-of-sight at a separation of (R) were used to determine the realized gain. They must be separated by a distance greater than or equal to $R = 2D^2/\lambda_0$, where D and λ are the antenna's greatest aperture dimensions and the wavelength for free space at the operating frequency f, in order to satisfy the far-field requirement. Power sent and received is denoted by Pt and Pr, respectively. Due to the similarities between the two antennas, the observed transmission coefficient from the VNA is represented by the power ratio Pr/Pt, where Gt is the transmitted gain and Gr the received gain, as seen in Equation (4). The miniaturized antipodal Vivaldi antenna resonates at 60 GHz with bandwidth of 4 GHz. This bandwidth performance can also be written in the percentage form, i.e., 7.3%, and the return loss is obtained at -64.73 dB. According to the radiation pattern measurement setup, a transmitting horn antenna is arranged in a coordinating configuration in line-of-sight with the tested antenna. The Standard Horn Antenna LB-19-20-C-1.85F has a low voltage standing wave ratio (VSWR) of $1.25 : 1$ and an output of 1.85 mm with a female connector. It operates between 40 GHz and 60 GHz with a nominal gain of 20 dBi.

The LB-19-20-C-1.85F model offers efficient performance characteristics and directionality due to its uniform gain over its frequency range. The standard gain-horn antenna is perfect

TABLE 4. Comparison between the previous and the proposed work.

Reference	Frequency Range (GHz)	Antenna Size (mm)	Peak Realized Gain (dBi)	Design Complexity	Substrate	Fabrication Technology	Applications
[3]	4–16	10.2 × 5	8.3	Simple	Taconic RF-45	PCB	Imaging system
[4]	3.5–5.3/8–12	1.85 × 1.40	15	Complex	RO4003C	PCB	5G
[5]	57–71	3 × 2.3	7	Complex	RO3003	PCB	5G
[9]	2.9–29.2	10.2 × 5	8.1	Simple	FR-4-Glass	PCB	wireless communication
[10]	5.5–20.82	3.85 × 2.78	9.3	Simple	Rogers 4350B	PCB	Remote sensing
[11]	22.5–45	5.5 × 12	8.5	Simple	Rogers 4350B	PCB	5G
[13]	3–4.5 THz	108 × 84	10.8	Complex	Graphene	Simulated only	IOT
[14]	3–10.6	36 × 36	8.5	Simple	FR-4	PCB	Microwave Imaging
[15]	20.04–25.5	25.6 × 7.9	8.2	Simple	Arlon AD430	PCB	Wireless communication
Proposed work	**58–62**	**2.5 × 5**	**12.9**	**Simple**	**FR-4**	**PCB**	**Mm-wave, Imaging**

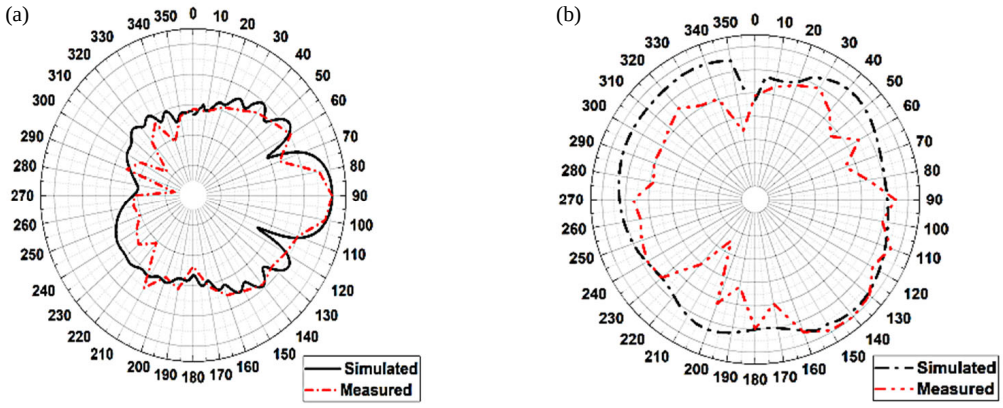

FIGURE 9. Simulated and measured radiation pattern for AVA antenna with directors at 60 GHz, (a) E-plane, (b) H-plane.

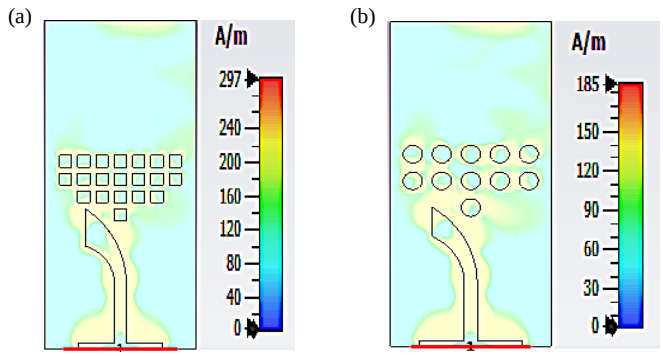

FIGURE 10. The current distribution for AVA antenna with directors, (a) square director, (b) circular director.

for measuring antenna gain and radiation pattern. The setup consists of a manual rotating rod fixed over a 360° protractor used for antenna under Test (AUT) mounting. Another fixed rod is positioned 20 cm away (to assure far-field operation) to mount the standard horn. The radiation pattern measurement process is accomplished by successively recording several data points at every 5° interval.

The AVA antenna generates a uniform and stable radiation pattern in the E-plane and H-plane also, exhibits superior side-lobe suppression throughout the bandwidth, as shown in Fig. 9. It can be noted that the agreement between the measured and simulated results is better. However, there are a few small differences between the simulated and measured values because of cable losses, defects in manufacturing, and other issues. The actual current distributed through the directors is induced in the

antenna by electromagnetic oscillations; this distributed current is responsible for the antenna pattern and the gain. The current is distributed through the antennas and director elements that increase the realized gain value, as shown in Fig. 10.

$$\frac{Pr}{Pt} = GtGr\left(\frac{\lambda_O}{4\pi R}\right)^2 \quad (4)$$

6. CONCLUSIONS

In this paper, miniaturized and compact antipodal Vivaldi antennas are designed and implemented on a low-cost FR-4 material with a 1.5-mm thickness. The antennas were designed using MWSCST tools to improve the gain. The antenna covers a millimeter-wave band from 58 GHz up to 62 GHz. This range is relevant to imaging and wireless applications. Circular and square director units are loaded on the AVA to increase the overall antenna gain. Directors fulfilled 3.68 dBi to the gain compared to the unloaded AVA. The finalized realized gain for an AVA without directors reached 9.22 dBi for modeling and 12.9 dBi for measurements. The antenna has a higher efficiency of up to 96%. The overall antenna gain has reached 12.9 dBi. The proposed AVA exhibits a stable and uniform radiation pattern. The proposed antenna appears to be an attractive choice for mm-wave communication applications.

ACKNOWLEDGEMENT

The authors express their thank and acknowledge the support from Universiti Teknikal Malaysia Melaka (UTeM), the Centre for Research and Innovation Management (CRIM), and the Ministry of Higher Education of Malaysia (MOHE).

REFERENCES

[1] Koga, Y. and M. Kai, "A transparent double folded loop antenna for IoT applications," in *2018 IEEE-APS Topical Conference on Antennas and Propagation in Wireless Communications (APWC)*, 762–765, Cartagena, Colombia, Sep. 2018.

[2] Hu, R., F. Zhang, S. Ye, and G. Fang, "Ultra-wideband and high-gain Vivaldi antenna with artificial electromagnetic materials," *Micromachines*, Vol. 14, No. 7, 1329, 2023.

[3] Ding, M., X. Wang, Y. Wang, Z. Hu, G. Liu, Z. Liu, and B. Wang, "A high gain Vivaldi antenna with multiple near-field dielectric lenses and grooved edges," *International Journal of RF and Microwave Computer-Aided Engineering*, Vol. 2023, Article ID 2405200, 2023.

[4] Cheng, H., H. Yang, J. Wu, Y. Li, Y. Fu, A. Zhang, and J. Jin, "Leaky-Vivaldi antenna covered with metasurface with leaky wave radiation and aperture radiation," *Optics Express*, Vol. 31, No. 11, 17 291–17 303, 2023.

[5] Ghaffar, F. A., N. K. Roy, and A. Shamim, "A single layer wideband Vivaldi antenna with a novel feed structure," *IET Microwaves, Antennas & Propagation*, Vol. 17, No. 7, 558–564, 2023.

[6] Rohaninezhad, M., M. J. Asadabadi, C. Ghobadi, and J. Nourinia, "Design and fabrication of a super-wideband transparent antenna implanted on a solar cell substrate," *Scientific Reports*, Vol. 13, No. 1, 9977, 2023.

[7] Nasir, M., A. Iftikhar, M. F. Shafique, B. Saka, S. Nikolaou, and D. E. Anagnostou, "Broadband dual-podal multilayer Vivaldi antenna array for remote sensing applications," *IET Microwaves, Antennas & Propagation*, Vol. 17, No. 7, 505–517, 2023.

[8] Azari, A., A. Skrivervik, H. Aliakbarian, and R. A. Sadeghzadeh, "A super wideband dual-polarized Vivaldi antenna for 5G mmWave applications," *IEEE Access*, Vol. 11, 80 761–80 768, 2023.

[9] Ibrahim, A. A. and S. M. Gaber, "Frequency reconfigurable antipodal Vivaldi 2-port antenna based on graphene for terahertz communications," *Optical and Quantum Electronics*, Vol. 55, No. 9, 786, 2023.

[10] Özmen, H. and M. B. Kurt, "A novel gain enhanced Vivaldi antenna for a breast phantom measurement system," *Electromagnetics*, Vol. 43, No. 1, 24–36, 2023.

[11] Yu, X., J. Li, J. Hu, Y. Yao, J. Li, and S. Yan, "Low-profile dual-polarized antenna integrated with horn and Vivaldi antenna in millimeter-wave band," *Applied Sciences*, Vol. 13, No. 17, 9627, 2023.

[12] Jaiswal, P. K., R. Bhattacharya, and A. Kumar, "A UWB antipodal Vivaldi antenna with high gain using metasurface and notches," *AEU — International Journal of Electronics and Communications*, Vol. 159, 154473, 2023.

[13] Tangwachirapan, S., W. Thaiwirot, and P. Akkaraekthalin, "Design and analysis of antipodal Vivaldi antennas for breast cancer detection," *Computers, Materials & Continua*, Vol. 73, No. 1, 411, 2022.

[14] Ibrahim, I. M., M. I. Ahmed, H. M. Abdelkader, and M. M. Elsherbini, "A novel compact high gain wide-band log periodic dipole array antenna for wireless communication systems," *Journal of Infrared, Millimeter, and Terahertz Waves*, Vol. 43, No. 11-12, 872–894, 2022.

[15] Zhao, C., Y. Bai, and Q. Wei, "A 2 to 50 GHz all-metal Vivaldi antenna for ultra-wideband (UWB) application," *AEU — International Journal of Electronics and Communications*, Vol. 148, 154162, 2022.

[16] Wang, J., J. Liu, Y. Fan, and Y. Bai, "A novel Vivaldi antenna for UWB detection," *Microwave and Optical Technology Letters*, Vol. 65, No. 3, 826–843, 2023.

[17] Paul, L. C. and M. M. Islam, "A super wideband directional compact Vivaldi antenna for lower 5G and satellite applications," *International Journal of Antennas and Propagation*, Vol. 2021, 1–12, 2021.

[18] Paik, H. and K. Premchand, "A compact antipodal Vivaldi antenna for modern surveillance systems," *International Journal of Electronics Letters*, 1–12, 2023.

[19] Rodas, A. E. and K. Ren, "A wideband Vivaldi antenna for drone-based microwave imaging system," in *ASEE-NE 2022*, Boston, MA, Apr. 2022.

[20] Dixit, A. S., S. Kumar, and M. Abegaonkar, "A corrugated and lens based miniaturized antipodal Vivaldi antenna for 28 GHz and 38 GHz bands applications," *Frequenz*, Vol. 77, No. 4, 475–484, Oct. 2023.

[21] Bhattacharjee, A., A. Bhawal, A. Karmakar, A. Saha, and D. Bhattacharya, "Vivaldi antennas: A historical review and current state of art," *International Journal of Microwave and Wireless Technologies*, Vol. 13, No. 8, 833–850, 2021.

[22] Sasikala, S., K. Karthika, S. Arunkumar, K. Anusha, S. Adithya, and A. J. A. Al-Gburi, "Design and analysis of a low-profile tapered slot UWB Vivaldi antenna for breast cancer diagnosis," *Progress In Electromagnetics Research M*, Vol. 124, 43–51, 2024.